RESEARCH ARTICLE | AUGUST 24 2022

Influence of encapsulation process temperature on the performance of perovskite mini modules

Sara Baumann ✉; Lukas Brockmann; Susanne Blankemeyer; ... et. al

AIP Conference Proceedings 2487, 120001 (2022)
https://doi.org/10.1063/5.0090632

Influence of Encapsulation Process Temperature on the Performance of Perovskite Mini Modules

Sara Baumann[1, a)], Lukas Brockmann[1], Susanne Blankemeyer[1], Verena Steckenreiter[1], Verena Barnscheidt[1], Marc Köntges[1], Sarah Kajari-Schröder[1], Sascha Jozsef Wolter[1], Henning Schulte-Huxel[1] and Tobias Wietler[1,2]

[1]*Institute for Solar Energy Research Hamelin (ISFH), Am Ohrberg 1, 31860 Emmerthal, Germany*
[2]*Institute for Electronic Materials and Devices, Leibniz University Hannover, Schneiderberg 32, 30167 Hannover, Germany*

[a)] Corresponding author: s.baumann@isfh.de

Abstract. Perovskite-on-silicon tandem solar cells are a promising candidate to significantly increase the efficiency of PV modules. Despite the fast research progress on material and solar cells aspects, there is still a lack of processes for an industrial module integration of these devices. One aspect hereby is the adaption of encapsulation materials and processes to the requirements of perovskite materials. Process temperatures of about 150 °C are necessary to use well proven, in silicon PV commonly applied encapsulation materials with a high reliability. However, perovskites start to decompose into their components at high temperatures. This limits the encapsulation process temperature, which in turn constraints the choice of encapsulation materials. This work presents an encapsulation process for methylammonium lead iodide ($MAPbI_3$) single junction perovskite solar cells (PSCs) with conventional production tools in glass-glass modules that serves as a model system for perovskite tandem applications. We evaluate the influence of the encapsulation process temperature between 120 °C and 160 °C on the performance of mini modules. The UV-absorbing encapsulation material is processable over the whole investigated temperature regime. We observe a difference in the *IV*-characteristics between the PSCs encapsulated in the temperature range of 120 °C – 140 °C to those processed at 160 °C. At lower encapsulation temperatures the *IV*-curves taken 1 h after encapsulation show a pronounced S-shape and no degradation of V_{OC}. In contrast, the PSCs encapsulated at 160 °C exhibit a V_{OC} decrease of up to 29% compared to the initial measurement shortly after PSC fabrication and no significant S-shape. Both, the S-shape that occurs at low encapsulation temperatures and the V_{OC} loss after encapsulation at 160 °C, are no longer significant after one week of module storage under dark conditions. The presented encapsulation process therefore does not permanently damage the $MAPbI_3$ PSCs even at a standard encapsulation temperature of 160 °C. To ensure long-term operation, we test the fabricated mini modules in a damp heat test at 85 °C and a relative humidity of 85%. We find no significant additional degradation caused by damp heat in 1250 h test duration compared to a reference module stored in ambient air.

INTRODUCTION

A key driver for reducing the cost of power generation by PV is to increase module efficiency, since the costs of PV systems are dominated by the balance of system cost and module materials that scale with module area. Perovskite-tandem solar cells with a silicon bottom cell are highly promising for reaching solar cell efficiencies beyond 30% [1] while being cost effective [2]. Module integration of this innovative cell type is an ongoing and important topic of research and is a prerequisite for their application [3]. A first perovskite-silicon-tandem module was recently introduced by OxfordPV [4] and Matteocci et al. reported the encapsulation of $MAPbI_3$ perovskite solar cells (PSCs) with curing glues and a thermo-plast processable at 100 °C instead of an encapsulation foil as commonly used in module processing of c-Si modules [2]. However, while there is a published module fabrication process with standard encapsulation materials like EVA or polyolefin for multi-cation-multi-anion PSCs [3], we found no such report for $MAPbI_3$.

SiliconPV 2021, the 11th International Conference on Crystalline Silicon Photovoltaics
AIP Conf. Proc. 2487, 120001-1–120001-8; https://doi.org/10.1063/5.0090632
Published by AIP Publishing. 978-0-7354-4362-4/$30.00

Perovskites degrade when exposed to high temperatures [5, 6], humidity [7] and UV-light [8]. This needs to be considered when developing encapsulation processes for PSCs. However, the usage of well-established materials and processes commonly used in silicon PV that need process temperatures of about 150 °C to 160 °C would facilitate a fast industrial application. In addition, it has the potential to be cost-effective since these materials are already being produced on large scale. Depending on the interconnection process a higher encapsulation temperature is also beneficial for the long-term stability of the electrical contacts. For their commercial realization PSCs need to be long-term stable under outdoor conditions which is ensured by passing international standards as for example IEC 61215 requesting long-term stability at 85 °C [5,9]. Therefore, the thermal stability of PSCs is of great importance.

Different temperature thresholds at which the structural change of $MAPbI_3$ starts are reported in the literature. Conings et al. observe significant structural changes in X-ray photoelectron spectroscopy (XPS) measurements already after annealing of $MAPbI_3$ at 85 °C in ambient atmosphere for 6 h. They indicate that XPS is very surface sensitive and the structural change is not homogenous. This might explain that the $MAPbI_3$ PSCs can still work properly even if they exhibit significant structural changes in XPS measurements [5]. Wolter et al. conducted X-ray diffraction (XRD) measurements, which in contrast to XPS rather map the bulk than the surface. They showed that $MAPbI_3$ is stable up to 135 °C for an annealing duration of several hours but decomposes into MAI and PbI_2 at above 140 °C [6]. The stability of $MAPbI_3$ in high-angle annular dark-field (HAADF) images up to 150 °C for 30 min is reported by Divitini et al. [10]. The HAADF images map a 150 nm thick cross section of a PSC.

We analyze the influence of encapsulation process temperatures between 120 °C and 160 °C on the performance of $MAPbI_3$ mini modules to evaluate whether standard encapsulation materials can be used for $MAPbI_3$ PSCs or alternative materials need to be investigated. With a damp heat test we analyze if moisture can ingress the fabricated glass-glass modules with a butyl edge sealing.

FABRICATION AND *IV*-CHARACTERIZATION OF PEROVSKITE MINI MODULES

The perovskite mini modules contain one substrate with four PSCs each as depicted in Fig. 1. The PSCs are separated by a laser-patterned 180 nm thick ITO layer on the 2.5 x 2.5 cm² glass substrate with a thickness of 0.7 mm. On top of the ITO layer we evaporate 10 nm spiro-TTB as a hole-transport layer (HTL), 500 nm $MAPbI_3$ as an absorber and 23 nm C60 + 8 nm BCP as an electron-transport layer (ETL) in p-i-n configuration. The $MAPbI_3$ absorber is deposited by co-evaporation of methylammonium iodide and lead iodide. The p- and n-side of the PSCs are both contacted with 100 nm thick evaporated Au pads. These Au contacts are connected with Cu wires with a low melting solder coating (T_{melt} = 118 °C) within the encapsulation process enabling the measurement of the PSCs in the module. In this way, we prepare modules with four individually contacted PSCs with an area of approx. 0.12 cm² each.

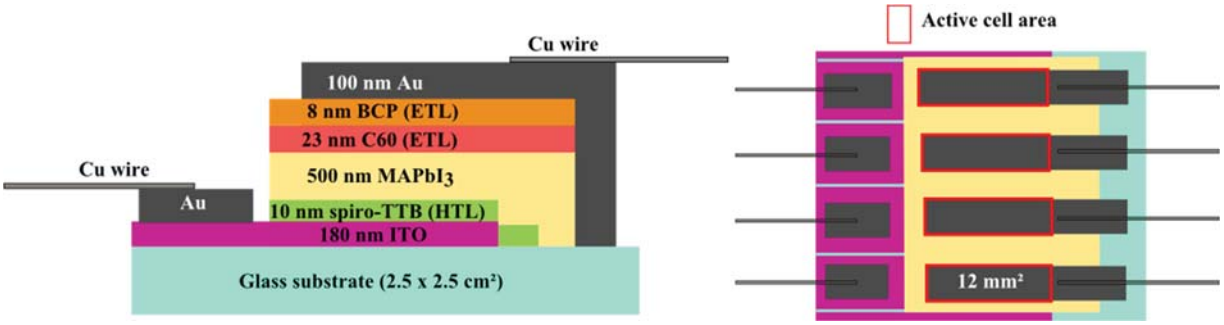

FIGURE 1. Cross section and top view of a substrate with four perovskite solar cells (PSCs) and their electrical contacting.

The PSCs are stored in a glove box with nitrogen atmosphere for about two months after their fabrication and initial measurement and before encapsulation. Contact needles in a four-point probe setup are used to connect the Au contacts of the bare PSCs before encapsulation. The encapsulated PSCs are measured by connecting the copper wires with the four-point probe in about 10 cm distance to the PSC. Due to the low current, series resistance is neglectable in these measurements. We measure the *IV*-curves at 25 °C under 1 sun illumination with an LED array simulating an AM1.5G spectrum shortly after PSC fabrication and within a few hours before, 1 h and one week after the encapsulation process. The PSCs have a short-circuit current I_{SC} of about 2 - 3 mA, an open-circuit voltage V_{OC} of about 1 V and an efficiency η of 10 – 12%.

We choose a polymeric encapsulation material with a processing temperature of below 120 °C and no need for high temperature curing in order to allow processing at lower temperatures compared to standard silicon PV. The encapsulation material absorbs wavelengths below 380 nm to protect the perovskite from UV-light. The modules have a 3 mm thick glass at the front and rear side and a butyl edge sealing to prevent moisture ingress. One glass substrate with four PSCs is embedded in the middle of each module with an area of 20 x 20 cm^2.

We encapsulate one substrate each at set process temperatures of 120 °C, 130 °C, 140 °C and 160 °C. The set encapsulation temperature T_{ENC} is always held for 12 min. The maximum actual temperature at the perovskite is about 5 °C lower than T_{ENC}. Due to three defect PSCs or incorrect measurements 13 PSCs are evaluated in total for the evaluation of the influence of T_{ENC} on the performance of perovskite mini modules (compare Table 1). Two substrates each are from the same perovskite process run, which means that they are evaporated and metallized together. The process runs all have the same set parameters.

For the damp heat test another two substrates of one fabrication process are encapsulated at 140 °C. One module with two intact PSCs (see Table 1) is thereby stored in ambient air under dark conditions as a reference. The average initial efficiency of the PSCs in both modules is similar ($\eta_{damp\ heat}$ = 12.3% ± 1.0% and $\eta_{reference}$ = 12.0% ± 1.0%). In the damp heat and the reference module all PSCs are measured before and after 5 min MPP tracking (MPPT). Thereby the applied voltage is varied in a small interval around the momentary V_{MPP} to follow P_{MPP}. Due to an error in the measurement algorithm, sometimes high reverse voltages and currents are applied to the PSC. The thereby dissipated power can cause a short-circuit of the corresponding PSC.

TABLE 1. Overview of the PSCs processed for the evaluation of the influence of T_{ENC} on PSC performance and the durability of the encapsulation to damp heat. PSC fabrication process 1, 2 and 3 are different evaporation and metallization processes with the same set parameters.

T_{ENC}	Perovskite process run	Number of PSCs
120 °C	1	2
130 °C	2	3
140 °C	2	4
160 °C	1	4
Damp heat (140 °C)	3	4
Reference (140 °C)	3	2

INFLUENCE OF THE ENCAPSULATION PROCESS TEMPERATURE ON THE PERFORMANCE PARAMETERS OF PEROVSKITE MINI MODULES

In this section we compare the solar cell parameters open-circuit voltage V_{OC}, short-circuit current I_{SC}, maximum power point P_{MPP} and fill factor *FF* as well as the form of the *IV*-characteristics of $MAPbI_3$ PSCs encapsulated at process temperatures in the range of 120 °C – 140 °C to those fabricated with a standard encapsulation temperature of 160 °C.

Results

Figure 2 (a) shows representative *IV*-curves for the PSCs of two different evaporation and metallization processes encapsulated in the low temperature regime (here: 130 °C) and Fig. 2 (b) for PSCs encapsulated at 160 °C, respectively. The PSCs encapsulated at 160 °C are from the same fabrication process as those encapsulated at 120 °C. In both cases we observe an I_{SC} decrease from the initial measurement shortly after PSC fabrication (lightblue solid curve) to the one after two months storage in nitrogen atmosphere directly before encapsulation (purple dotted line). V_{OC} does not change significantly.

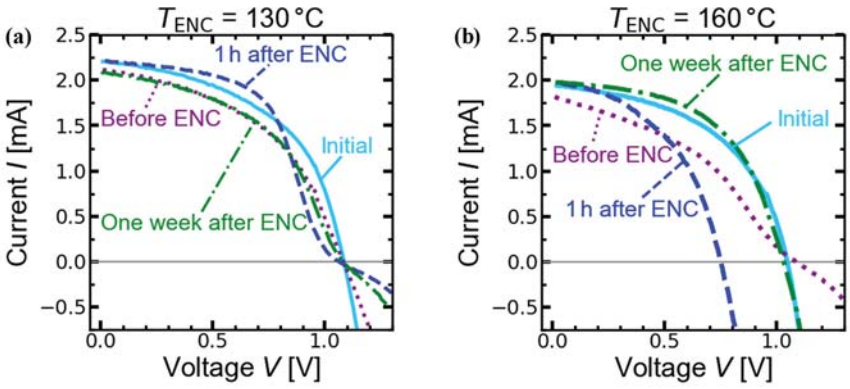

FIGURE 2. Representative *IV*-characteristics of a PSC encapsulated at 130 °C (a) which is exemplary for the range of 120 °C – 140 °C and at 160 °C (b). The PSCs were stored in nitrogen atmosphere for two months between the initial measurement (blue solid line) and the one taken shortly before encapsulation (purple dotted line). This causes an I_{SC} decrease in 9/13 PSCs which can be regenerated by encapsulation (see dark blue dashed line). The dark blue dashed lines also show the pronounced S-shape at process temperatures in the range of 120 °C – 140 °C (a) and the V_{OC} decrease 1 h after encapsulation at 160 °C (b). Both effects are regenerated after one week of storage under dark conditions (see dash-dotted green curve).

Figure 3 shows relative I_{SC} values for all processed PSCs before encapsulation (purple), 1 h (blue) and one week after encapsulation (green) compared to initial. As you can see from the purple dots I_{SC} has decreased in 9/13 PSCs after two months storage in nitrogen atmosphere directly before encapsulation by on average -8.4% ± 3.8%. After the encapsulation the loss in I_{SC} due to the storage in these nine PSCs is recovered (before MPPT) and lies within ± 5% of the initial measured I_{SC} for all PSCs (see blue dots).

Three of the four PSCs which do not show an I_{SC} decrease after storage and increase after encapsulation have a relatively constant I_{SC} after storage (purple squares) and encapsulation (blue squares) with deviations smaller than 3.5% of the initial value. Only one PSC (encapsulated at 140 °C) exhibits an I_{SC} increase by 5% after storage (purple pentagon) and a 5% decrease in relation to the initial measurement after encapsulation (blue pentagon).

The *IV*-curves of the samples encapsulated at T_{ENC} in the range of 120 – 140 °C show an S-shape in the *IV*-characteristics of all PSCs, which is depicted in Fig. 2 (a) by the dashed dark blue curve. In contrast, all samples prepared at T_{ENC} equal to 160 °C show an exponential rising *IV*-curve and a V_{OC} loss in the measurement taken 1 h after encapsulation (see Fig. 3 (b)).

From the green dash-dotted curve in Fig. 2 (a) you can see that the S-shape is significantly less pronounced after one week of dark storage of the PV modules. The V_{OC} loss in case of an encapsulation at 160 °C also regenerates within one week of dark module storage (compare Fig. 2 (b)).

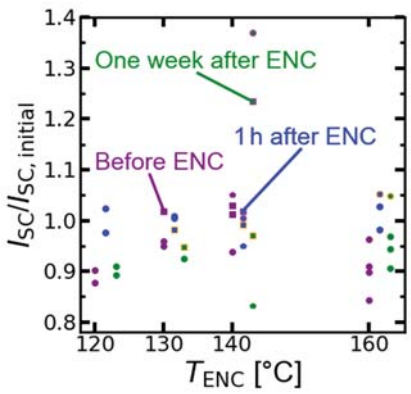

FIGURE 3. Relative I_{SC} after two months storage in nitrogen (purple), 1 h (blue) and one week after encapsulation (green) to initial.

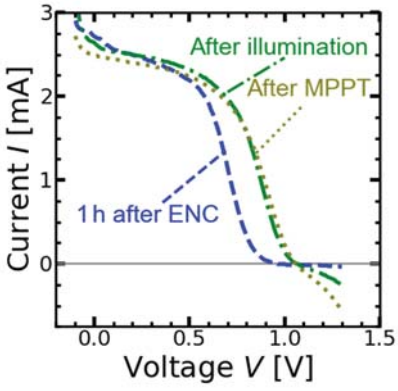

FIGURE 4. Diminishing of the S-shape in a similar way as shown in Fig. 2 (a) by 1 sun illumination 1 h after encapsulation at 140 °C and stabilized *IV*-curve after 5 min of MPPT.

Figure 4 shows that illumination at 1 sun for about 10 min reduces the S-shape after encapsulation (at 140 °C) in a similar way as the storage for one week under dark conditions (compare the dashed blue to the dash-dotted green line). No further changes in the *IV*-characteristics occur after subsequent maximum power point (MPP) tracking (MPPT) of the module for 5 min (see dotted olive green line).

As mentioned above the decrease of I_{SC} by -8.4% ± 3.8% in 9/13 PSCs due to storage in nitrogen atmosphere for two months between initial measurement and the one taken shortly before encapsulation is partially or even fully regenerated (± 5% of initial measurement) after encapsulation. However, one week later I_{SC} again decreased to a value comparable to that before encapsulation in eight PSCs (green markers in Fig. 3 without framing) as for example shown in Fig. 2 (a) whereas it stays in the regime of the initial value as the one depicted in Fig. 2 (b) for only three PSCs (framed orange). For the remaining two PSCs I_{SC} is increased after one week storage of the modules in the dark compared to the measurement shortly after encapsulation (framed pink). We thereby do not observe any dependence of I_{SC} on the encapsulation process temperature.

Figure 5 (a) shows relative values for V_{OC} resulting from the ratio of the measurement one hour (blue dots) and one week (green squares) after encapsulation to the initial one taken shortly after PSC fabrication in dependence of the encapsulation process temperature. With one exception all PSCs encapsulated at 120 °C – 140 °C exhibit a change in V_{OC} of maximum ± 4%. In contrast, V_{OC} of the four PSCs on the substrate encapsulated at 160 °C is 1 h after encapsulation decreased by 6% - 29%. However, one week of dark storage regenerates the V_{OC} loss. This results in a mean deviation from the initial measurement of only -3% and is thus highly comparable with the average relative V_{OC} after encapsulation at 140 °C (see Table 2). Therefore, our encapsulation process does not permanently damage $MAPbI_3$ PSCs even at a standard encapsulation temperature of 160 °C.

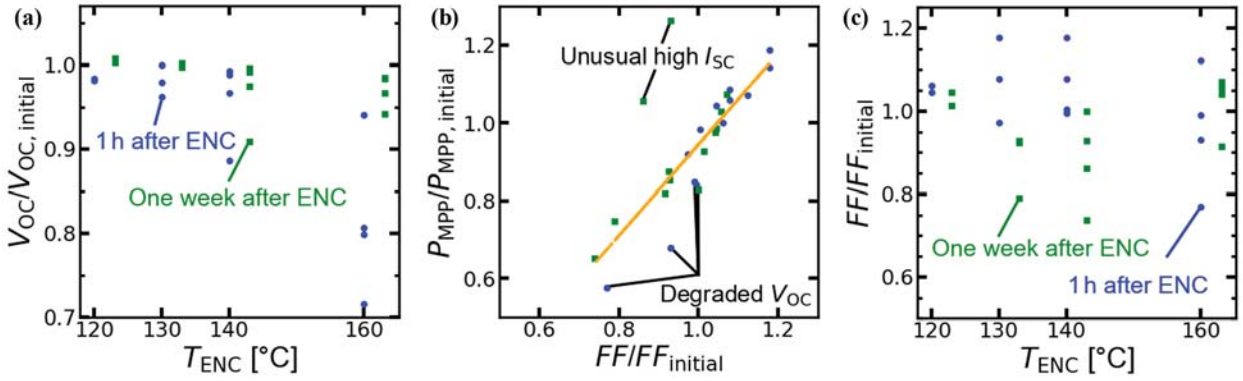

FIGURE 5. (a) Relative V_{OC} values compared to the initial measurement show a significant V_{OC} decrease and regeneration for the PSCs encapsulated at 160 °C, whereas V_{OC} stays within ± 4% for the PSCs encapsulated at lower temperatures with one exception. (b) High correlation of relative P_{MPP} with relative *FF* for 1 h and one week after encapsulation visualized by the orange guide to the eye despite of some exceptions. (c) Relative *FF* compared to initial show no significant temperature dependence but might be influenced by PSC processing.

In Fig. 5 (b) relative P_{MPP} values of both, the measurement 1 h (blue dots) and one week (green squares) after encapsulation, are plotted over the corresponding relative fill factors *FF*. Since most datapoints are close to the linear guide to the eye (orange line), relative P_{MPP} is highly correlated with relative *FF* 1 h as well as one week after encapsulation. The measurements that deviate significantly either have a large V_{OC} loss (five PSCs, compare Fig. 5 (a)) or an unusual high I_{SC} (two PSCs, compare pink framed green markers in Fig. 3) one week after encapsulation (at 140 °C). Thus, we cannot expect a linear correlation between P_{MPP} and *FF* for these PSCs as V_{OC} and I_{SC} respectively influence P_{MPP} in this case. However, we conclude that in general P_{MPP} mainly depends on *FF*.

As depicted in Fig. 5 (c) the relative *FF* is widely distributed and shows no significant dependence on the encapsulation temperature 1 h as well as one week after encapsulation. The PSCs on the substrates encapsulated at 120 °C and 160 °C and at 130 °C and 140 °C respectively were evaporated and Au metallized together. As we know that especially the metallization influences the performance of the PSCs, the higher *FF* decrease during one week storage of the PSCs on the substrates encapsulated at 130 °C and 140°C compared to the other two might rather be influenced by PSC processing than by the encapsulation process.

TABLE 2. Average V_{OC} deviation from $V_{OC,\,initial}$ 1 h and one week after encapsulation for all investigated encapsulation process temperatures.

Average V_{OC} deviation from $V_{OC,\,initial}$	120 °C	130 °C	140 °C	160 °C
1 h after ENC	-1.7%	-1.9%	-4.1%	-18.4%
One week after ENC	+0.9%	-0.1%	-3.2%	-3.1%

Discussion

The I_{SC} of a module measured with a black cover on the measurement chuck and a mask exposing only the perovskite absorber to light is comparable to the measurement with full illumination of the module. This means that I_{SC} is not increased by light scattered at the glass substrate or the chuck due to back reflections at the front side glass. Ray-tracing simulations with the software Sunrays [11] yield a 7% lower current density within the module stack compared to the bare PSC due to optical losses in the encapsulation materials.

Thus, the measured increase in I_{SC} after encapsulation is not caused by additional light reflections in the module but can be attributed to an improvement in current generation of the PSC. This conclusion is supported by the regeneration of I_{SC} of a bare PSC after 5 min of MPP tracking (not shown here). The observation of an increased $MAPbI_3$ crystallinity in XRD measurements after annealing up to 120 °C by Wolter et al. [6] gives reason to assume the encapsulation process being an annealing effect resulting in a higher I_{SC} after encapsulation. In contrast to our results Coletti et al. [12] report a lowering in I_{SC} of perovskite tandem solar cells at comparable encapsulation temperatures. They observe a regeneration of I_{SC} only after several hours of MPP tracking.

The difference of the PSC behavior at an encapsulation temperature in the range of 120 °C – 140 °C and at 160°C might be explained with the XRD measurements of Wolter et al. [6]. As the temperature of the PSC during encapsulation is about 5 °C lower than the set process temperature reached on the outside of the module, the set temperature T_{ENC} = 140 °C corresponds to a temperature of 135 °C in the XRD measurements. At this temperature the PbI_2 peak is not yet visible and the $MAPbI_3$ is therefore assumed to be still intact. At 160 °C the decomposition into MAI and PbI_2 should have begun according to the XRD measurements. However, the XRD measurements were conducted with a $MAPbI_3$ layer without contact layers and an Au metallization as the PSCs in this work have. Bush et al. report that an ITO capping layer can prevent the egress of MAI and thus increases the thermal stability of $MAPbI_3$ PSCs [13]. The Au contact pads might have a similar effect. An alternative explanation for the PSCs withstanding higher encapsulation temperatures than expected might be given by Conings et al. They state that the decomposition of $MAPbI_3$ occurs much more slowly in the absence of oxygen and water [5]. Ideally, this is the case inside of a solar module.

The regeneration of a V_{OC} loss in $MAPbI_3$ PSCs as large as shown above has not been reported before as far as we know. However, Divitini et al. also observed a decrease in V_{OC} of about 20% in $MAPbI_3$ PSCs at 90 °C and ascribed it to increased charge carrier recombination maybe influenced by iodine vacancies [9]. In addition, they report an irreversible degradation of light conversion properties above 90 °C, but do not specify whether the V_{OC} decrease after annealing belongs to the irreversible properties or not.

The decrease of V_{OC} is not necessarily caused by the decomposition of $MAPbI_3$ but could also be explained by changes in the carrier transport layers or interfaces as the PSC is for instance heated above the glass transition temperature of spiro-TBB of 146 °C [14]. The origin of the V_{OC} degeneration during encapsulation and its regeneration, which might be accelerated by illumination (see Fig. 4), is currently under investigation.

EVALUATION OF THE DURABILITY OF THE ENCAPSULATION TO DAMP HEAT

To evaluate the durability of the above described module fabrication process we conduct the ISOS-D-3 damp heat test as defined in [15] following the international standard IEC 61215 at 85% RH and 85 °C. We therefore encapsulate two substrates of the same fabrication process at 140 °C as mentioned in Table 1.

Figure 6 (a) shows the relative efficiency of the module tested with damp heat and the reference after certain hours of damp heat duration in relation to the measurement shortly after encapsulation. Hereby the efficiency after 5 min of MPP tracking is evaluated. It can be seen that the damp heat module does not show significant degradation compared to the reference module within the large fluctuations up to a test duration of 1250 h. We conclude that the module is sufficiently sealed by the butyl sealant and that our encapsulation material and process parameters are suitable to protect the PSCs from moisture.

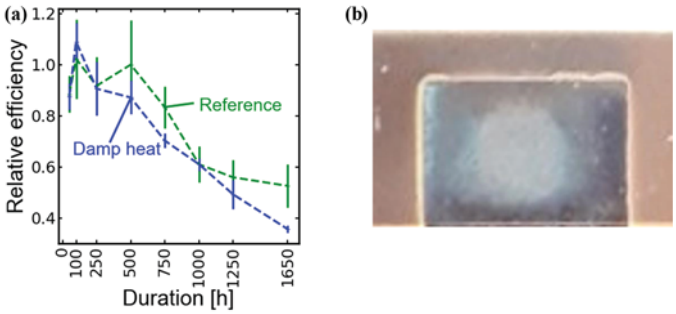

FIGURE 6. (a) Relative Efficiency over damp heat duration for the damp heat and the reference module stored in air at RT under dark conditions. Both modules have a similar initial efficiency ($\eta_{damp\ heat}$ = 12.31% ± 1.01% and $\eta_{reference}$ = 11.98% ± 1.05%). (b) Discoloration of the active PSC area after an incorrect MPP tracking which short-circuited the corresponding PSC.

Notice that two cells of the damp heat module were short-circuited by MPP tracking during the experiment (one after 250 h and the other after 1250 h, compare Table 3). Relatively high currents of about 140 mA and reverse bias voltages of about -3 V and thus about - 400 mW were dissipated during the MPP tracking. Figure 6 (b) depicts the discoloration of the active PSC area that was observed after such an MPP tracking. The electrical contacting of another PSC of the damp heat module is broken between 750 h and 1000 h test duration so that the PSC cannot be measured anymore even though it might still be intact. After 1650 h damp heat a yellow coloring of the $MAPbI_3$ layer outside of the active solar cell area is observed.

TABLE 3. Overview of the evaluated PSCs and failures in the damp heat and reference module during damp heat test (DH).

Module label	Cell number	Failures
Damp heat	1	
	2	Broken contact before measurement after 1000 h DH
	3	Short-circuited after MPPT after 250 h DH
	4	Short-circuited after MPPT after 1250 h DH
Reference	1	
	2	

However, the degradation of the test sample in the damp heat test is comparable to the reference for 1250 h damp heat test. That suggests a sufficient sealing by the butyl edge and that the degradation is caused by something other than the damp heat test. As the reference module is stored at room temperature, temperature alone is probably also not the reason for the degradation. An influence of the *IV*-measurement or MPP tracking on the degradation mechanism cannot be excluded so far. The efficiency of the PSCs in the reference module can be regenerated to 85.9% ± 1.8% of their initial value by illumination with 1 sun for 140 min. The module is heated to about 63 °C during the illumination and the efficiency stays constant after 140 min dark storage. Further experiments are planned to clarify the origin of the PSC discoloration and the decrease in efficiency of both the reference and the damp heat module over time.

CONCLUSION

From XRD measurements we expect the decomposition of $MAPbI_3$ into MAI and PbI_2 at encapsulation process temperatures above 140 °C. Indeed, we observe a difference in mini modules encapsulated at temperatures below this threshold compared to the one at a temperature of 160 °C. At low encapsulation process temperatures the *IV*-characteristics 1 h after encapsulation exhibit a pronounced S-shape whereas V_{OC} is decreased 1 h after encapsulation at 160 °C by on average 18.43% ± 8.02%. Both features regenerate during one week dark storage. This means that the encapsulation temperature of the presented process causes no permanent damage in our $MAPbI_3$ PSCs even with standard encapsulation temperatures. This enables the use of well-established cheap encapsulation materials known from silicon PV and might simplify the industrial implementation of PSCs. In addition, the fabricated glass-glass modules with a butyl edge sealing are found to be suitable to prevent additional PSC degradation induced by humidity and high temperatures in a damp heat test conducted for more than 1000 h.

ACKNOWLEDGMENTS

Authors thank the German Federal Environmental Foundation (DBU), the state of Lower Saxony and the Federal Ministry for Economic Affairs and Energy (BMWi) under grant number 03EE1017B (P3T) for their funding and M. Diederich, M. Löhning, Y. Larionova, J. Strey and M. C. Turcu (all from ISFH) for PSC processing.

REFERENCES

1. B. C. Duck *et al*., "Energy yield potential of perovskite-silicon tandem devices", *2016 IEEE 43rd Photovoltaic Specialists Conference (PVSC)*: 1624-1629, Portland, OR, USA (2016)
2. F. Matteocci *et al.*, "Encapsulation for long-term stability enhancement of perovskite solar cells", *Nano Energy* **30**: 162-172 (2016)
3. F. Corsini *and* G. Griffini, "Recent progress in encapsulation strategies to enhance the stability of organometal halide perovskite solar cells", *J. Phys. Energy* **2** (2020)
4. B. Williams *et al.*, "Quantifying Bottlenecks in Open-Circuit Voltage of Perovskite-Si Tandem Solar Cells", *36th EU PVSEC* (2020).
5. B. Conings *et al*., "Intrinsic Thermal Instability of Methylammonium Lead Trihalide Perovskite", *Adv. Mater.* **5**: 1500477 (2015)
6. S. J. Wolter *et al.*, "Dual-Source Co-Evaporation of Perovskite Absorbers and Determination of the Acoustic Impedance Ratio of the Deposited Single Precursors", *MRS Fall Meeting* (2017)
7. J. Yang *et al.*, "Investigation of $CH_3NH_3PbI_3$ degradation rates and mechanisms in controlled humidity environments using in situ techniques", *ASC Nano* **9**: 1955–1963 (2015)
8. S.-W. Lee *et al.,* "UV degradation and recovery of perovskite solar cells", *Sci. Rep.* **6**: 38150 (2016)
9. Q. Meng *et al.*, "Effect of temperature on the performance of perovskite solar cells", *J. Mater. Sci.: Mater. Electron.* (2020)
10. G. Divitini *et al*., "In situ observation of heat-induced degradation of perovskite solar cells", *Nature Energy* **1** (2016)
11. R. Brendel, "Sunrays: A Versatile Ray Tracing Program for the Photovoltaic Community", *12th European photovoltaic solar energy conference* (1994)
12. G. Coletti *et al.*, "Scaling Up Four-Terminal Bifacial Tandem", *36th EU PVSEC* (2020).
13. K. A. Bush *et al*., "Thermal and Environmental Stability of Semi-Transparent Perovskite Solar Cells for Tandems Enabled by a Solution-Processed Nanoparticle Buffer Layer and Sputtered ITO Electrode", *Adv. Mater.* **28**: 3037-3943 (2016)
14. C. Murawski *et al*., "Alternative p-doped hole transport material for low operating voltage and high efficiency organic light-emitting diodes", *Appl. Phys. Lett.* **105**: 113303 (2014)
15. M. V. Khenkin *et al*. „Consensus statement for stability assessment and reporting for perovskite photovoltaics based on ISOS procedures", *Nature Energy* **5**: 35–49 (2020)